*Maejo Int. J. Sci. Technol.* **2026**, *20*(03), 284-299

***Maejo International Journal of Science and Technology***

**e-ISSN 2697-4746**
Available online at www.mijst.mju.ac.th

***Full Paper***

# Cellular immunity in *Periplaneta americana* exposed to bio-synthesised AgNPs from *Bacillus cereus* group strain CS3

**Berfin Dilekci [1], Ayse S. Saygi [1], Ebru G. Ozkorkmaz [2], Hakan Eskizengin [1], Nur K. Kilic [1] and Nursel Gul [1, *]**

[1] Department of Biology, Faculty of Science, Ankara University, 06100 Tandogan, Ankara, Turkey
[2] Faculty of Health Sciences, Ankara Yildirim Beyazit University, 06760 Cubuk, Ankara, Turkey
* Corresponding author, e-mail: ngul@science.ankara.edu.tr

*Received: 13 April 2026 / Accepted: 27 October 2026 / Published: 28 October 2026*

**Abstract:** The cellular response of hemocytes in *Periplaneta americana* to silver nanoparticles (AgNPs), synthesised by *Bacillus cereus* group strain CS3 was investigated. AgNPs with an average diameter of 12.5 ± 3.3 nm were administered to the insects and the resulting hemocyte-mediated cellular and morphological responses were examined. AgNPs doses of 0.02, 0.04 and 0.06 mg/g body weight were applied to 5$^{th}$-stage nymphs of *P. americana*. Hemolymph samples were collected from nymphs at 1, 4, 72 hr and 1 week after application, stained with Giemsa, then observed under light microscope. Control hemocyte samples exhibited normal cell structure and no immune reactions were observed. Upon application of 0.02 mg/g AgNPs, hemocytes contacted each other, forming aggregations and nodular structures. At 0.04 mg/g dose, hemocytes, particularly plasmatocytes, were observed to establish contact through cytoplasmic extensions, resulting in hemocyte aggregation and nodule formation. Moreover, AgNP exposure was associated with morphological alterations including chromatin loss in the nuclei of hemocytes and cytoplasmic vacuolisation. At highest AgNP concentration (0.06 mg/g), both hemocyte aggregation and nodule formation were consistently observed. These findings demonstrate that exposure to the synthesised AgNPs induces hemocyte-mediated cellular responses, i.e. nodulation and hemocyte aggregation, together with morphological alterations indicative of cellular stress in *P. americana*.

**Keywords:** silver nanoparticles, *Periplaneta americana*, *Bacillus cereus* group strain CS3, hemocytes, immune response, nanotoxicology

*Maejo Int. J. Sci. Technol.* **2026**, 20(03), 284-299

## INTRODUCTION

*Periplaneta americana* (Linnaeus, 1758), also known as American cockroach, is a pest inhabiting warm and humid environments and commonly found in human settlements [1]. Due to its rapid development, high fertility and remarkable tissue regeneration capacity, it is considered a valuable hemimetabolous model organism in biological research [2]. The insect immune system relies entirely on innate immunity and consists of humoral and cellular components [3, 4]. Humoral responses include antimicrobial peptide production and the generation of reactive oxygen and nitrogen species through cascades regulating coagulation and melanisation in the hemolymph [5, 6].

Cellular immunity is mediated by hemocytes and is rapidly activated upon pathogen exposure [7]. It primarily involves phagocytosis/pinocytosis, nodulation and encapsulation [5, 7, 8]. Nodulation occurs against microorganisms such as bacteria, fungi and protozoa, where hemocytes aggregate to form microclusters that trap and eliminate pathogens [9-11]. Encapsulation, in contrast, targets larger invaders such as parasitoids and nematodes by forming multilayered hemocyte structures [11-13]. This process is associated with hemocyte aggregation, partial cell disintegration and activation of the prophenoloxidase cascade, leading to melanisation and the production of reactive oxygen and nitrogen species [8]. Together, nodulation and encapsulation represent key defense mechanisms that localise and eliminate invading pathogens [8].

In recent year numerous studies have investigated the effects of nanoparticles on insects [14-19]. Among them, silver nanoparticles (AgNPs) have attracted significant attention due to their high surface-to-volume ratio, ease of functionalisation, antimicrobial activity and cytotoxic properties. AgNPs can be synthesised using physical, chemical and biological methods [20]. However, physical and chemical approaches often require high energy input, elevated temperatures and toxic reagents, posing environmental and health risks as well as cost limitations [21].

Biological synthesis has therefore emerged as a more sustainable and cost-effective alternative, utilising microorganisms or plant-derived compounds as reducing and stabilising agents. Numerous studies have demonstrated the biological effects of AgNPs on insects. For instance, AgNPs exhibited lethal effects on *Blattella germanica* [22] and induced morphological changes in the hemocytes of *Bombyx mori* [23]. In *Aedes aegypti* AgNPs exposure resulted in increased oxidative stress and apoptosis [16] while in *Drosophila melanogaster* enhanced defense responses were reported [24]. Additionally, AgNP-based formulations have been shown to affect gut microbiota, immune responses and survival of various insect species including *Spodoptera litura*, *Spodoptera exigua* and *Galleria mellonella* [25-28]. Plant- and microbe-derived AgNPs have also demonstrated insecticidal activity against species such as *Helicoverpa armigera* and *Periplaneta americana* [29, 30].

In this study silver nanoparticles were synthesised using the indigenous *Bacillus cereus* group strain CS3 isolated from municipal landfill leachate in Sanliurfa,Turkey.The synthesised AgNPs were characterised and their effects on the hemocytes of *Periplaneta americana* were evaluated at different doses and exposure periods. Particular attention was given to hemocyte-mediated cellular responses, i.e. nodulation and hemocyte aggregation as well as morphological alterations associated with cellular stress. Thus, the study focuses on the dose- and time-related hemocyte responses of *P. americana* to biogenic AgNP exposure while also demonstrating the use of a waste-derived local bacterial isolate as a biological source for AgNP synthesis.

*Maejo Int. J. Sci. Technol.* **2026**, 20(03), 284-299

## MATERIALS AND METHODS

### Bacterium and Biogenic AgNP Synthesis

The indigenous bacterial strain CS3, isolated from municipal landfill leachate in Sanliurfa, Turkey, was obtained from the culture collection of Bioremediation Research Laboratory, Department of Biology, Faculty of Science, Ankara University. For AgNPs production, CS3 was grown in 100 mL nutrient broth medium for 3 days. At the end of the incubation period, centrifugation was performed at 6000 rpm for 10 min. The supernatant (5 mL) was transferred to a 1 mM $AgNO_3$ solution (45 mL) in brown bottles. This mixture was incubated at 37 °C at 150 rpm with shaking for 24 hr [31]. Following synthesis, the AgNPs were collected by centrifugation at 10,000 rpm for 10 min. (Hermle Z207A, Germany), dried at 70°C overnight and resuspended in distilled water to prepare a stock suspension of 10 mg/mL.

### Polymerase Chain Reaction (PCR) and Sequencing

Bacterial identification was conducted through amplification of the 16S ribosomal DNA (rDNA) gene. For this purpose, 3 µL of bacterial suspension was directly introduced into the PCR mixture without a preceding DNA extraction step. The hypervariable V3–V4 regions of the 16S rDNA were selectively amplified using the universal primer pair 341F and 805R, following a previously established protocol [32]. PCR reactions were performed under optimised thermal cycling conditions consisting of an initial denaturation at 95 °C for 3 min., followed by 35 amplification cycles of denaturation at 95 °C for 20 s, annealing at 57 °C for 25 s and extension at 72 °C for 50 s. A final extension step was carried out at 72 °C for 5 min. to ensure complete amplification of the target fragments.

### Characterisation of AgNPs

*UV-Visible spectrophotometric analysis*

The optical properties of the biogenically synthesised AgNPs were analysed using a UV-Vis spectrophotometer (BioDrop, UK). The absorption spectra of the nanoparticle suspension were recorded within the wavelength range of 300–600 nm. A 1 mM $AgNO_3$ solution was used as the blank for the UV-Vis measurements.

*Transmission electron microscopy (TEM)*

The morphology and size distribution of the synthesised AgNPs were examined using a transmission electron microscope (JEOL JEM 100 CXII, Japan). The particle diameters were determined by analysing at least 100 measurement points with ImageJ software (version 1.53n).

*Attenuated total reflection fourier transform infrared spectroscopy (ATR-FTIR)*

For ATR-FTIR measurements, 5 µL of each sample was used. The spectra were recorded with a spectrometer (Thermo-Scientific, Nicolet iS50, USA) equipped with an ATR accessory (ConcentratIR2, Harrick, USA) with ten internal reflections. Prior to measurement, the samples were dried under a gentle stream of $N_2$ gas for 15 min. to remove excess water. The previously prepared AgNPs powder was placed directly on the ATR diamond crystal. Absorbance spectra were collected by averaging 120 scans at a resolution of 4 $cm^{-1}$. ATR correction was performed using the OMNIC software (version 8.2.388) and the spectra were used for visualisation without any further

preprocessing. Difference spectra were generated by subtracting two area-normalised absorbance spectra, where area normalisation was applied to minimise the effects of concentration differences. The subtraction factor was interactively adjusted until the resulting spectrum exhibited positive and negative peaks distributed around the zero baseline.

**Insect Culture**

*Periplaneta americana* specimens were obtained from an established laboratory culture maintained at the Animal Ecology Laboratory, Department of Biology, Ankara University. The insects were reared under controlled conditions at 26 ± 2°C and 60 ± 5% relative humidity with a 12-hr dark/light photoperiod [33]. Throughout the experimental period, they were provided with biscuits and water ad libitum. $5^{th}$-stage nymph individuals of *P. americana* were used in the experiments. Ethical approval was not required for this study as the experiments were conducted on an invertebrate species.

**Application of AgNPs to Insects**

At each time point, five insects were examined per experimental group. The experimental design consisted of four groups (one control group and three AgNP-treated groups), four exposure periods and five insects per group at each time point, resulting in a total of 80 insects (4 groups × 4 time points × 5 insects). The cockroaches were held between the thumb and index finger, with the ventral side facing upwards and the posterior end directed towards the syringe. Subsequently, AgNPs was injected into the last two abdominal sternites close to the lateral margin, using a 27G fine-tip hypodermic syringe (1 mL) [34, 35]. The body weight of fifth-instar nymphs was estimated to be approximately 1 g per insect. Accordingly, AgNP doses of 0.02, 0.04 and 0.06 mg/g body weight were administered by injecting 2, 4 and 6 µL of the AgNP suspension per insect respectively. Control insects received the corresponding volume of sterile saline solution. The dose selection was based on the study by El-Samad et al. [35].

**Collection and Preparation of Hemolymph from Insects**

Hemolymph samples were collected at 1, 4, 72 hr and 1 week after exposure. The hemolymph was extracted from the ventral side of the cockroach. To access the hemolymph, the metathoracic leg was bent toward the head, exposing a membrane at its base. A sterile needle was used to puncture this membrane, creating an opening. A 5-µL micropipette was then carefully inserted into the opening at a horizontal angle and the hemolymph was drawn by applying gentle pressure [34]. A portion of the collected hemolymph was smeared onto a slide, air-dried and subsequently stained using Giemsa Stain (Merck). After a one-minute staining period, the slides were rinsed with distilled water, dried and mounted with Entellan (Merck). Cellular immune responses of cockroach hemocytes were examined using a light microscope (Olympus BX43, Japan) and independently evaluated by two blinded histopathologists.

**Histopathological Scoring**

A semi-quantitative histopathological scoring approach was used to evaluate cellular responses according to AgNP dose and exposure duration. The severity of histopathological alterations was graded using a five-point scoring scale: 0 = no change, 1 = minimal, 2 = mild, 3 = moderate and 4 = marked. For each experimental condition, histopathological parameters were

evaluated across ten distinct microscopic fields and the mean score was calculated. The resulting semi-quantitative scores were used descriptively to compare patterns of cellular alterations across AgNP doses and exposure periods and were not subjected to inferential statistical analysis.

## RESULTS

### Identification of Isolate CS3

Bacterial isolate CS3 was characterised by amplification and sequencing of the 16S rRNA gene. Basic Local Alignment Search Tool for nucleotides analysis and sequence comparison revealed that strain CS3 shares 98.86% sequence identity with several members of the *Bacillus cereus* group. Therefore, strain CS3 is assigned to the *B. cereus* group.

Phylogenetic relationships are reconstructed using the neighbour-joining method [36]. Evolutionary distances are estimated using the maximum composite likelihood method [37] and are expressed as the number of base substitutions per site. Ambiguous positions are removed from each sequence pair using the pairwise deletion option, resulting in a final dataset of 304 positions. All evolutionary analyses are conducted using MEGA11 [38]. The resulting phylogenetic tree is presented in Figure 1. In the reconstructed tree, strain CS3 clusters most closely with *Bacillus paramycoides* strain PM51, supporting its placement within the *B. cereus* group. The partial 16S rRNA gene sequence of strain CS3 was deposited in the NCBI GenBank database under accession number PX313667.

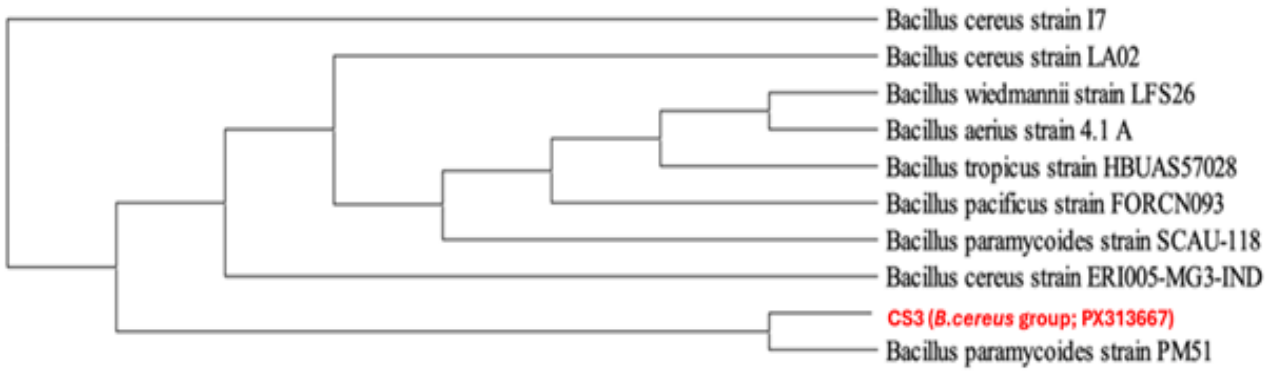



**Figure 1.** Phylogenetic tree of CS3 strain

### Characterisation of AgNPs

*UV-Visible spectrophotometric analysis*

During the synthesis process, the development of a characteristic brown coloration provided an initial indication of AgNP formation. Extracellular nanoparticle synthesis was evaluated by recording the UV-Vis spectra of the reaction mixture at predetermined intervals over the wavelength range of 300–600 nm. An absorption band centered at approximately 428 nm was observed, consistent with the characteristic surface plasmon resonance of AgNPs [39] (Figure 2).

*Maejo Int. J. Sci. Technol.* **2026**, 20(03), 284-299

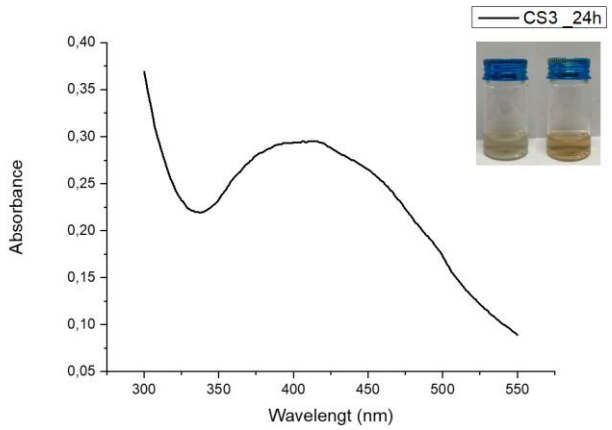



**Figure 2.** UV-visible spectrum of AgNPs

*TEM analysis*

The morphology of the AgNPs synthesised at 37°C is analysed using TEM. Micrographs reveal that the nanoparticles produced using the cell-free supernatant predominantly exhibit a spherical shape. In the samples incubated at 37°C for 24 hr, the average particle size is determined to be 12.5 ± 3.3 nm (Figure 3).

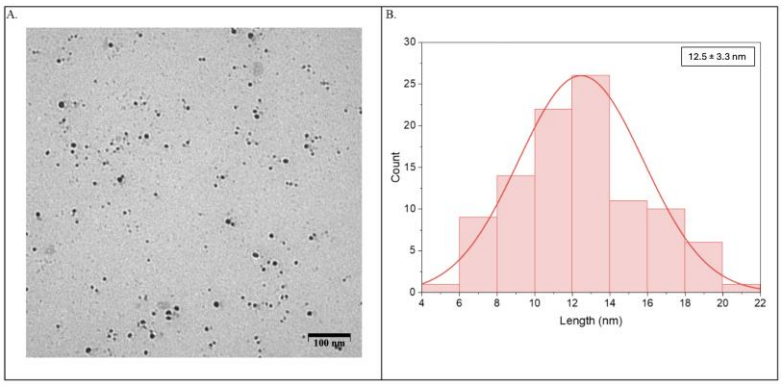



**Figure 3.** (A) TEM image of AgNPs; (B) Particle size distribution of AgNPs

*FTIR analysis*

The FTIR spectrum indicates the presence of functional groups that may be associated with biomolecules involved in nanoparticle capping and stabilisation [40]. The broad absorption band around 3200-3550 $cm^{-1}$ corresponds to O–H stretching vibration, indicating the presence of hydroxyl groups (Figure 4). Peaks in the range of ~2300–2100 $cm^{-1}$ are attributed to C≡N or C≡C stretching, which suggests the involvement of proteins, amino acids or alkyne groups in the capping process. The distinct peak between 1626-1662 $cm^{-1}$ may be assigned to C=C stretching vibration, suggesting the possible presence of alkene-related functional groups. Additionally, the low-frequency band around 610 $cm^{-1}$ may be associated with C–Cl stretching vibration [41].

*Maejo Int. J. Sci. Technol.* **2026**, 20(03), 284-299

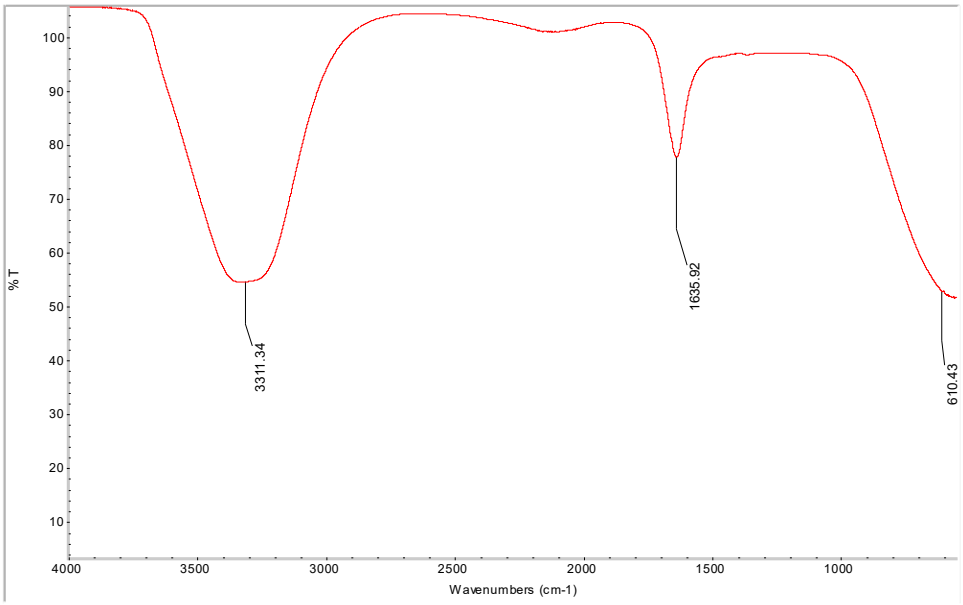



**Figure 4.** FTIR analysis of AgNPs

## Cellular Immunity Observations

To evaluate the effects of nanoparticles on hemocyte morphology, hemolymph samples from untreated and exposed insects were examined. Hemocytes in the control group exhibit normal structural characteristics under light microscopy (Figure 5A). To assess cellular immune responses and cellular stress-related alterations, hemolymph samples were analysed across different doses and exposure times. One hr after exposure to 0.02 mg/g AgNPs, hemocytes show intercellular contact via cytoplasmic extensions, along with localised chromatin disintegration in some nuclei (Figure 5B). Small nodular aggregations are also observed (Figure 5C). At 4 hr after exposure, hemocytes are closely associated, with evident nodule formation and distinct nodular structures consistent with a cellular immune response (Figures 5D, E). After 72 hr, pronounced hemocyte aggregation is observed, with multiple hemocytes forming closely associated cellular clusters (Figures 5F, G). This is accompanied by cellular stress-related alterations, i.e. cytoplasmic material loss, vacuole formation and chromatin depletion in some nuclei (Figure 5G). One week after exposure, nodular structures and hemocyte aggregations are evident (Figure 5H). Several hemocytes also exhibit nanoparticle-induced morphological alterations including nuclear changes and chromatin loss.

One hr after administration of 0.04 mg/g AgNPs, examination of hemolymph samples reveals that hemocytes are clustered together, with some established direct contact and formed nodular structures (Figure 6A). Four hr after administration, light microscopy reveals multiple nodular structures predominantly formed by plasmatocytes (Figures 6B, C). Seventy-two hr after administration, both nodular structures and pronounced hemocyte aggregations are observed (Figures 6D, E). In addition, several hemocytes exhibit cellular stress-related alterations, i.e. cytoplasmic vacuolisation and changes in nuclear morphology, particularly chromatin loss (Figures 6D, E). One week after administration, hemocytes remain aggregated; however, distinct nodular structures are less evident than at earlier time points (Figure 6F).

*Maejo Int. J. Sci. Technol.* **2026**, 20(03), 284-299

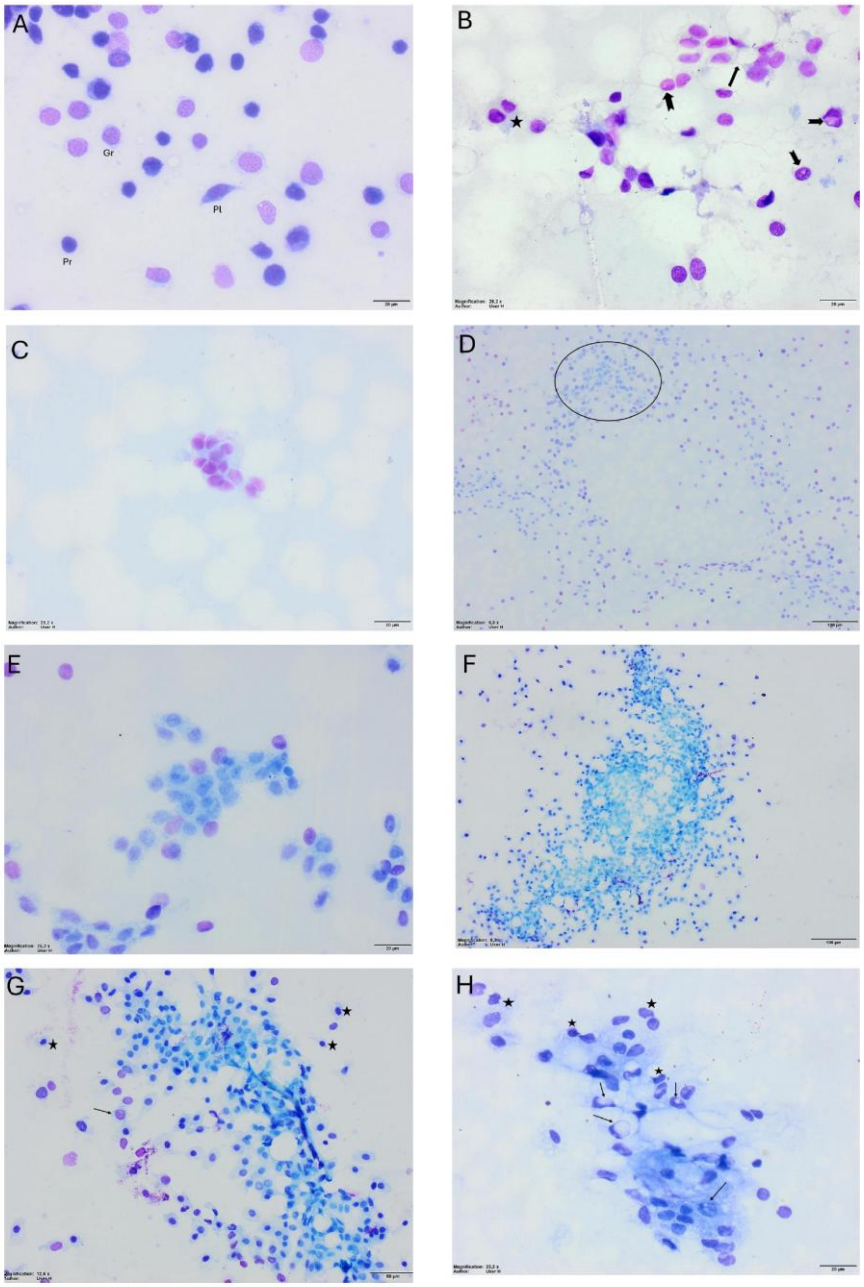



**Figure 5.** Giemsa-stained hemocytes showing morphology, cellular immune responses and cellular stress-related alterations in *Periplaneta americana* following exposure to 0.02 mg/g AgNPs : (A) Hemocytes of control group – plasmatocyte (Pl), granulocyte (Gr) and prohemocyte (Pr) (×400). (B–C) Hemocyte alterations at 1 hr after exposure. (B) Cells in contact with each other (star), cytoplasmic extensions (arrow) and chromatin loss in nuclei (arrowhead) (×400). (C) Nodule formation (×400). (D–E) Cellular immune responses at 4 hr after exposure. (D) Cells in contact with each other and nodule structure (circle) (×100). (E) Nodule structure formed by aggregated hemocytes (×400). (F–G) Hemocyte aggregation and cellular stress-related alterations at 72 hr after exposure. Hemocyte aggregation, vacuolisation and cytoplasmic material loss in hemocytes (star) and nuclear chromatin loss (arrow) (F ×100, G ×200). (H) Hemocyte alterations at 1 week after exposure. Nodule structure with altered nuclear morphology (star) and cellular material loss (arrow) (×400).

*Maejo Int. J. Sci. Technol.* **2026**, 20(03), 284-299

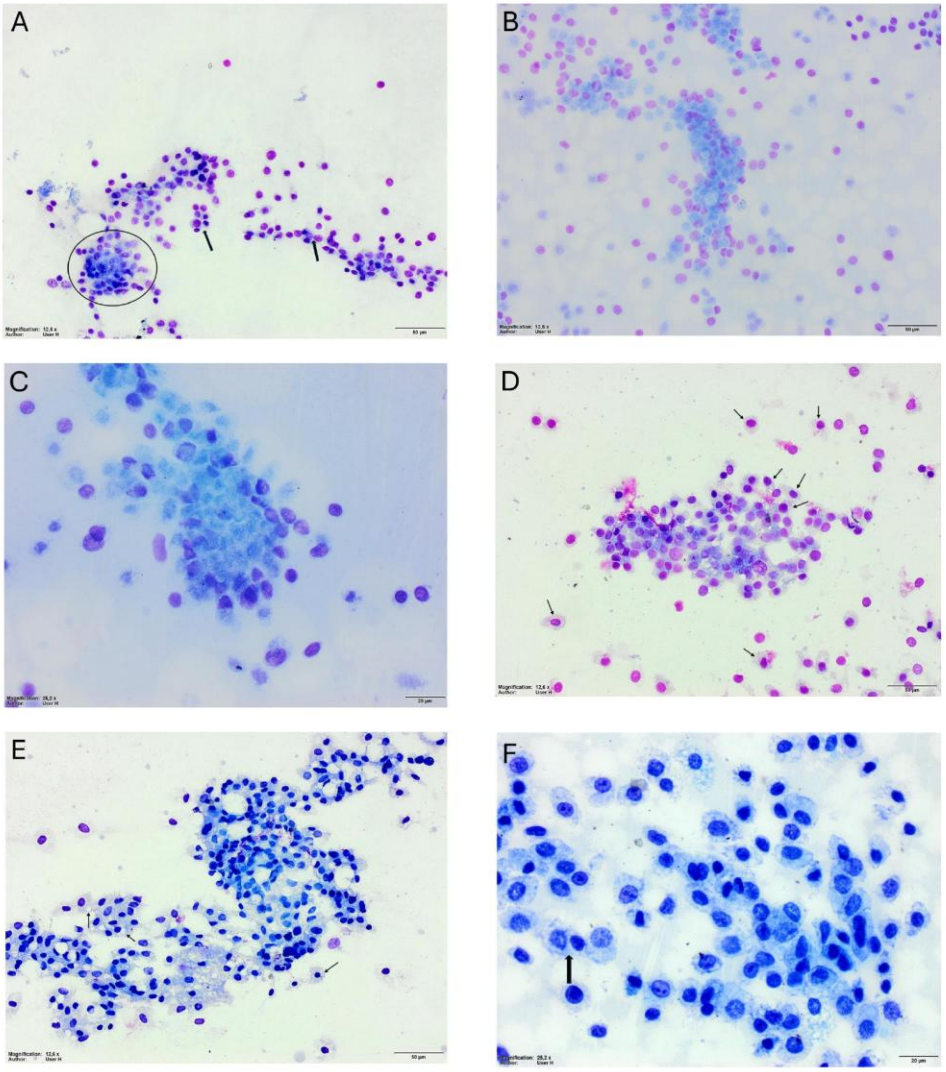



**Figure 6.** Giemsa-stained hemocytes showing morphology, cellular immune responses and cellular stress-related alterations in *Periplaneta americana* following exposure to 0.04 mg/g AgNPs : (A) Hemocyte alterations at 1 hr after exposure. Hemocytes in contact with each other (arrow) and nodule structure (circle) (×200). (B–C) Cellular immune responses at 4 hr after exposure. Nodule structures formed by aggregated hemocytes (B ×200, C ×400). (D–E) Hemocyte aggregation and cellular stress-related alterations at 72 hr after exposure. (D) Nodule structure and cytoplasmic vacuolisation in hemocytes (arrow) (×200). (E) Pronounced hemocyte aggregation and cytoplasmic vacuolisation in hemocytes (arrow) (×200). (F) Hemocyte aggregation and membrane disruption (arrow) at 1 week after exposure (×400).

One hr after administration of the highest experimental dose of AgNPs (0.06 mg/g), microscopic examination of hemolymph samples reveals that hemocytes form small aggregates, establish intercellular contact and form nodular structures (Figure 7A). Four hr after administration, hemocytes remain in close intercellular contact and form distinct nodular structures (Figure 7B). Seventy-two hr after administration, hemocytes similarly exhibit intercellular contact and nodular aggregation (Figure 7C). One week after administration, hemocytes remain aggregated and in close intercellular contact; however, distinct nodular structures are not observed at this time point. Vacuole formation is also observed (Figure 7D).

*Maejo Int. J. Sci. Technol.* **2026**, 20(03), 284-299

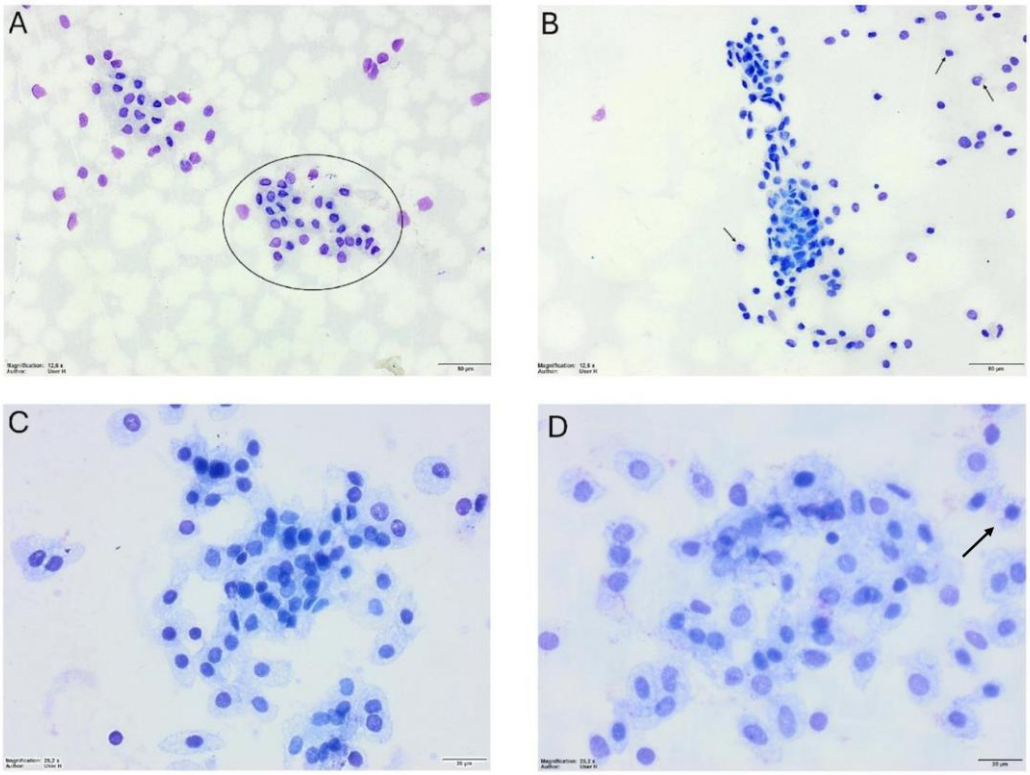



**Figure 7.** Giemsa-stained hemocytes showing morphology, cellular immune responses and cellular stress-related alterations in *Periplaneta americana* following exposure to 0.06 mg/g AgNPs : (A) Hemocytes in close intercellular contact and nodule formation (circle) at 1 hr after exposure (×200). (B) Hemocytes in close intercellular contact and nodule formation at 4 hr after exposure. Disruption of membrane integrity is also observed in some hemocytes (arrow) (×200). (C) Nodule formation at 72 hr after exposure (×400). (D) Hemocyte aggregation and intercellular contact at 1 week after exposure with cytoplasmic vacuolisation (arrow) (×400).

## Histopathological Scoring

Semi-quantitative histopathological scoring reveals variations in cellular alterations across AgNP doses and exposure periods (Figure 8). Compared with the control group, AgNP-exposed groups show higher scores for several histopathological parameters, i.e. nodule formation, abnormal hemocyte morphology, hemocyte aggregation, cytoplasmic vacuolisation, chromatin loss and disruption of membrane integrity. At the highest AgNP dose (0.06 mg/g), the most pronounced alterations are observed at 1 week with abnormal hemocyte morphology, chromatin loss and disruption of membrane integrity, each reaching a score of 4. Cytoplasmic vacuolisation and hemocyte aggregation also exhibit variations in their scoring profiles across the evaluated exposure periods. Overall, the semi-quantitative scoring profiles reveal distinct patterns of cellular alterations across different AgNP doses and exposure periods as illustrated in Figure 8.

*Maejo Int. J. Sci. Technol.* **2026**, 20(03), 284-299

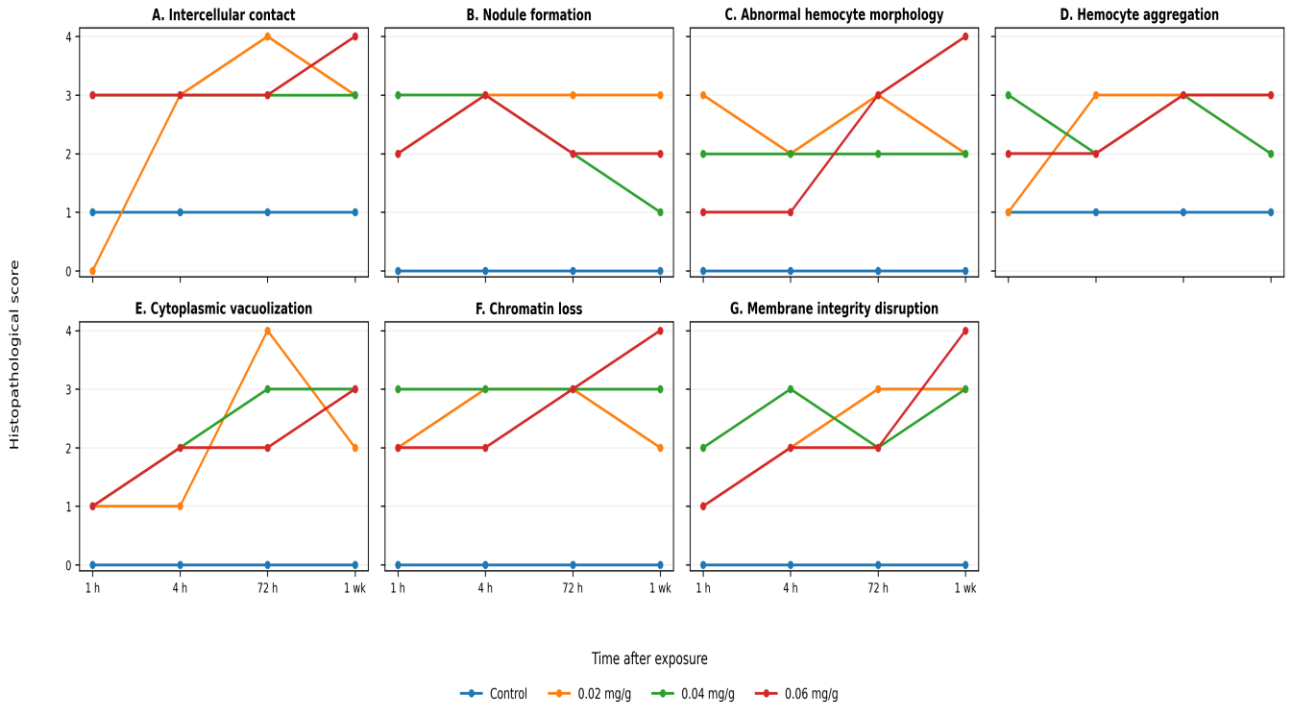



**Figure 8.** Semi-quantitative histopathological scoring of hemocyte responses following AgNP exposure. Histopathological scores for cellular alterations in the control and AgNP-treated groups (0.02, 0.04 and 0.06 mg/g) at 1, 4, 72 hr and 1 week after exposure. Scores represent the mean values obtained from ten microscopic fields for each experimental condition.

## DISCUSSION

The green synthesis of AgNPs using *Bacillus* species has previously been reported. Ahmed et al. [42] synthesised AgNPs ranging from 18 to 39 nm using *B. cereus* SZT1 while Kabeerdass et al. [43] produced AgNPs with an average diameter of 40.2 nm using *Bacillus* strain mn14. Previous studies have also demonstrated insect-related effects of AgNPs including alterations in the hemocyte morphology of *Bombyx mori* [23], tissue damage in *Blaps polychresta* [35] and insecticidal activity against *Periplaneta americana* using plant-derived AgNPs [30]. In contrast, the present study used an indigenous *Bacillus cereus* group strain isolated from municipal landfill leachate in Sanliurfa, Turkey and focused specifically on the dose- and time-related hemocyte responses of *P. americana*. Thus, the contribution of this study lies in characterising nodulation, hemocyte aggregation and associated hemocyte morphological alterations following exposure to AgNPs synthesised using a waste-derived indigenous bacterial isolate.

The formation of AgNPs is supported by the characteristic surface plasmon resonance band observed in the UV–Vis spectrum while TEM provides information on particle morphology and size, and FTIR indicates the presence of functional groups potentially associated with nanoparticle capping and stabilisation. However, energy-dispersive X-ray spectroscopy and X-ray diffraction analyses were not performed in the present study. Therefore, direct elemental confirmation of silver and characterisation of the crystalline structure of the nanoparticles could not be provided. This represents a limitation of the present study and should be addressed in future studies.

In recent years nanoparticles have received increasing attention because of their potential applications in various fields including insect control. Accordingly, several studies have investigated their effects on insect survival, cellular responses and immune-related parameters. Gad

[23] reported that different concentrations of AgNPs alter cell morphology and cause structural changes in the hemocytes of *Bombyx mori*. In particular, irregularities in the cell membrane, reduced cytoplasmic volume and vacuole formation in granulocytes are observed. Similarly, in the present study morphological alterations, i.e. cytoplasmic vacuolisation, changes in nuclear morphology and chromatin loss, are observed in some hemocytes following AgNP exposure. These alterations may reflect cellular stress or cytotoxic effects associated with AgNP exposure.

Luo and Wang [44] investigated the toxic effects of AgNPs on the hemocytes of the oyster *Crassostrea hongkongensis* and reported that granulocytes were the most affected cell type. AgNP exposure was also associated with increased reactive oxygen species production in granulocytes, impaired lysosomal function and reduced phagocytic activity. In the present study morphological alterations are similarly observed in hemocytes following AgNP exposure. In addition, hemocyte aggregation and nodular structures are observed at several exposure times. These morphological findings may be associated with cellular immune responses to AgNP exposure.

Andirin et al. [28] investigated the antioxidant and immunotoxic effects of AgNPs synthesised using *Ceratonia siliqua* on last-instar *Galleria mellonella* larvae. AgNP exposure resulted in changes in antioxidant and nervous system enzyme activities, total hemocyte count and phenoloxidase activity, indicating oxidative stress and immunotoxic effects in *G. mellonella*. Consistent with the reported cellular effects of AgNP exposure, structural alterations are also observed in some hemocytes in the present study.

Demirturk et al. [18] reported that exposure of *G. mellonella* larvae to metallic alumina and polystyrene nanoparticles negatively affects hemocyte functions and reduced immune-related responses, i.e. encapsulation, melanisation and phenoloxidase activity. Namasivayam and Bharani [25] investigated immune responses to an AgNP-loaded pyrrole-based pesticide metabolite in the lepidopteran pest *Spodoptera litura*. They reported reductions in hemocyte number and phenoloxidase production and suggested an immunosuppressive effect associated with weak lectin expression. In the present study hemocyte aggregation and nodular structures are observed following AgNP exposure. Although these morphological findings may be associated with cellular immune responses, direct conclusions regarding immune activation or suppression cannot be drawn because quantitative immune parameters were not evaluated. Likewise, the observed vacuolisation, chromatin loss and cytoplasmic alterations may reflect cellular stress or cytotoxicity rather than immune activation.

The possible contribution of $Ag^+$ ions released from the AgNPs should also be considered when interpreting the observed cellular responses. As dissolved $Ag^+$ concentrations were not measured and an ionic-silver control was not included, the effects observed in the hemocytes cannot be attributed exclusively to the particulate form of silver. Future studies should quantify $Ag^+$ release and compare AgNP exposure with an appropriate $AgNO_3$ control to distinguish nanoparticle-specific effects from those caused by dissolved silver ions.

Nanoparticles have been investigated as potential tools for pest management; however, their efficacy, target specificity, toxicity, biodegradability and long-term environmental effects require further evaluation.

## CONCLUSIONS

This study demonstrates the potential of an indigenous *Bacillus cereus* group strain isolated from municipal landfill leachate in Turkey as a microbial resource for the green synthesis of AgNPs. Exposure of *Periplaneta americana* nymphs to the synthesised AgNPs produces distinct

hemocyte-mediated cellular responses, i.e. intercellular contact, nodulation and hemocyte aggregation. Morphological alterations such as cytoplasmic vacuolisation, chromatin loss and disruption of membrane integrity further indicate that AgNP exposure is associated with cellular stress in addition to immune-related responses. These findings provide new insights into the interactions between biogenic AgNPs and the cellular defense system of *P. americana*.

The study also provides a biological basis for further investigation of waste-derived microbial AgNPs in pest management research. Future studies incorporating mortality, survival, development and reproductive endpoints will determine whether the observed cellular effects translate into practical pest-control efficacy.

**ACKNOWLEDGEMENTS**

Part of the study was presented as a poster presentation (P-10) in 7th International Environmental Chemistry Congress Environchem, December 2025, Istanbul, Turkey. Thanks are due to the participants for their valuable contributions.

**REFERENCES**

1. S. Li, S. Zhu, Q. Jia, D. Yuan, C. Ren, K. Li, S. Liu, Y. Cui, H. Zhao, Y. Cao, G. Fang, D. Li, X. Zhao, J. Zhang, Q. Yue, Y. Fan, X. Yu, Q. Feng and S. Zhan, “The genomic and functional landscapes of developmental plasticity in the American cockroach", *Nat. Commun.*, **2018**, *9*, Art.no.1008.
2. W. J. Bell and K. G. Adiyodi (Ed.), "The American Cockroach", Chapman and Hall, London, **1981**.
3. P. Bulet, R. Stöcklin and L. Menin, "Anti-microbial peptides: from invertebrates to vertebrates", *Immunol. Rev.*, **2004**, *198*, 169-184.
4. M. Kloc, M. Halasa, J. Z. Kubiak and R. M. Ghobrial, "Invertebrate immunity, natural transplantation immunity, somatic and germ cell parasitism, and transposon defense", *Int. J. Mol. Sci.*, **2024**, *25*, Art.no.1072.
5. M. D. Lavine and M. R. Strand, "Insect hemocytes and their role in immunity", *Insect Biochem. Mol. Biol.*, **2002**, *32*, 1295-1309.
6. A. Zdybicka-Barabas, S. Stączek, M. Kunat-Budzyńska and M. Cytryńska, "Innate immunity in insects: The lights and shadows of phenoloxidase system activation", *Int. J. Mol. Sci.*, **2025**, *26*, Art.no.1320.
7. I. Eleftherianos, C. Heryanto, T. Bassal, W. Zhang, G. Tettamanti and A. Mohamed, "Haemocyte-mediated immunity in insects: Cells, processes and associated components in the fight against pathogens and parasites", *Immunol.*, **2021**, *164*, 401-432.
8. I. M. Dubovskiy, N. A. Kryukova, V. V. Glupov and N. A. Ratcliffe, "Encapsulation and nodulation in insects", *Invertebr. Surviv. J.*, **2016**, *13*, 229-246.
9. H. Tunaz, "Mechanism of insect immunity", *KSU J. Sci. Eng.*, **2004**, *7*, 78-82.
10. J. L. Ding, J. Hou, M. G. Feng and S. H. Ying, "Transcriptomic analyses reveal comprehensive responses of insect hemocytes to mycopathogen Beauveria bassiana and fungal virulence-related cell wall protein assists pathogen to evade host cellular defense", *Virulence*, **2020**, *11*, 1352-1365.
11. N. Gul and C. Ayvali, “Purification and determination of the molecular structure of hemolymph lectin of *Agrotis segetum* (Denis and Schiff.)”, *Turk. J. Biol.*, **2002**, *26*, 49-55.

12. R. F. Chapman, "The Insects: Structure and Function", 4th Edn., Cambridge University Press, Cambridge, **1998**, pp.124-126.
13. A. S. Gandhe, S. H. John and J. Nagaraju, "Noduler, a novel immune up-regulated protein mediates nodulation response in insects", *J. Immunol.*, **2007**, *179*, 6943-6951.
14. J. D. Judy, J. M. Unrine, W. Rao and P. M. Bertsch, "Bioaccumulation of gold nanomaterials by *Manduca sexta* through dietary uptake of surface contaminated plant tissue", *Environ. Sci. Technol.*, **2012**, *46*, 12672-12678.
15. R. A. Bharani and S. K. R. Namasivayam, "Biogenic silver nanoparticles mediated stress on developmental period and gut physiology of major lepidopteran pest *Spodoptera litura* (Fab.) (Lepidoptera: Noctuidae)—An eco-friendly approach of insect pest control", *J. Environ. Chem. Eng.*, **2017**, *5*, 453-467.
16. N. Mehmood, A. Hassan, X. Zhong, Y. Zhu, G. Ouyang, T. Raza, S. Zia, X. Chen and Q. Huang, "Entomopathogenic fungi-based silver nanoparticles: A potential substitute of synthetic insecticides to counter behavioral and physiological immunity in *Aedes aegypti* mosquito (Diptera: Culicidae)", *Environ. Sci. Pollut. Res.*, **2024**, *31*, 30793-30805.
17. Z. Wang, N. Fan, X. Li, L. Yue, X. Wang, H. Liao and Z. Xiao, "Trophic transfer of metal oxide nanoparticles in the tomato-*Helicoverpa armigera* food chain: Effects on phyllosphere microbiota, insect oxidative stress and gut microbiome", *ACS Nano*, **2024**, *18*, 26631-26642.
18. Z. Demirturk, F. Uckan and S. Mert, "Interactions of alumina and polystyrene nanoparticles with the innate immune system of *Galleria mellonella*", *Drug Chem. Toxicol.*, **2024**, *47*, 483-495.
19. J.A. Gutiérrez-Ramírez, R. Betancourt-Galindo, L. A. Aguirre-Uribe, E. Cerna-Chávez, A. Sandoval-Rangel, E. C. Ángel, J. C. Chacón-Hernández, J. I. García-López and A. Hernández-Juárez, "Studying the insecticidal effect of titanium oxide nanoparticles on the *Periplaneta americana*", *Entomol. Appl. Sci. Lett.*, **2024**, *11*, 40-47.
20. S. Iravani, H. Korbekandi, S.V. Mirmohammadi and B. Zolfaghari, "Synthesis of silver nanoparticles: Chemical, physical and biological methods", *Res. Pharm. Sci*., **2014**, *9*,385-406.
21. S. Hosny, L. Z. Mohamed, M. S. Ragab, Q. K. Alomoush, E. M. Abdalla and S. A. Aly, "Nanomaterials in biomedical applications: Opportunities and challenges—a review", *Chem. Pap*., **2025**, *79*, 2657-2678
22. A. M. Abd El-Raheem and B. M. Eldafrawy, "Efficacy of Silver Nanoparticles against German Cockroach *Blattella germanica* (L.)(Dictyoptera: Blattellidae)", *Acad. J. Entomol.,* **2016**, *9*, 74-80.
23. A. A. Gad, "Toxicity effect of silver nanoparticles to the haemocytes and antioxidant activity of silkworm *Bombyx mori*", *Physiol. Entomol.*, **2020**, *45*, 154-160.
24. Z. Wang, L. Zhang and X. Wang, "Molecular toxicity and defense mechanisms induced by silver nanoparticles in *Drosophila melanogaster*", *J. Environ. Sci.*, **2023**, *125*, 616-629.
25. S. K. R. Namasivayam and R. S. A. Bharani, "Silver nanoparticles loaded pyrrole based pesticidal metabolites (AgNps-PFM) nanoconjugate induced impact on the gut microbion and immune response against lepidopteron pest *Spodoptera litura* (Fab.)" *Indian J. Biochem. Biophys*., **2021**, *58*, 478-485.
26. P. S. Araújo, M. B. Caixeta, A. Canedo, E. da Silva Nunes, C. Monteiro and T. L. Rocha,"Toxicity of plant-based silver nanoparticles to vectors and intermediate hosts: Historical review and trends", *Sci. Total Environ.*, **2022**, *834*, Art.no.155299.

27. Y. Sanjaya, A. Fitriani and A. M. Firdausa, "Bioinsecticide activity of silver nanoparticles product of biosynthesis using entomopathogen against the beet caterpillar *Spodoptera exigua*", *J. Biopestic.*, **2022**, *15*, 26-30.
28. A. Andirin, N. D. Yayci, M. Idikut, A. Kara, M. Tuncsoy, B. Tuncsoy and P. Ozalp, "Green synthesis of silver nanoparticles using carob leaf extract: Characterization and analysis of toxic effects in model organism *Galleria mellonella* L. (The greater wax moth)", *Environ. Sci. Pollut. Res. Int.*, **2024**, *31*, 57778-57788.
29. S. U. R. Qamar, S. Tanwir, W. A. Khan, J. Altaf and J. N. Ahmad, "Biosynthesis of silver nanoparticles using *Ocimum tenuiflorum* extract and its efficacy assessment against *Helicoverpa armigera*", *Int. J. Pest Manage.*, **2024**, *70*, 375-383.
30. O. A. Olaniran, J. A. Elegbede, A. Lateef, T. A. Adebayo, E. B. Gueguim-Kana, L. S. Beukes, N. Matyumza and F. O. Alao, "Anti-cockroach activities of biosynthesized silver nanoparticles using *Petiveria alliacea* extracts", *Beni-Suef Univ. J. Basic Appl. Sci*., **2025**, *14*, Art.no.23.
31. N. O. S. Keskin, N. K. Kilic, G. Donmez and T. Tekinay, "Green synthesis of silver nanoparticles using cyanobacteria and evaluation of their photocatalytic and antimicrobial activity", *J. Nano Res.*, **2016**, *40*, 120-127.
32. L. W. Hugerth, H. A. Wefer, S. Lundin, H. E. Jakobsson, M. Lindberg, S. Rodin, L. Engstrand and A. F. Andersson, "DegePrime, a program for degenerate primer design for broad-taxonomic-range PCR in microbial ecology studies", *Appl. Environ. Microbiol.*, **2014**, *80*, 5116-5123.
33. R. Y. Chai and C. Y. Lee, "Insecticide resistance profiles and synergism in field populations of the German cockroach (Dictyoptera: Blattellidae) from Singapore", *J. Econ. Entomol.*, **2010**, *103*, 460-471.
34. J. J. B. Smith, "Determining hemolymph volume of the cockroach", in "Tested Studies for Laboratory Teaching (Ed. C. A. Goldman), Vol. 15, Proceedings of 15th Workshop/Conference of the Association for Biology Laboratory Education, Atlanta (GA), USA, **1994**, pp.119-139.
35. L. M. El-Samad, N. R. Bakr, S. El-Ashram, E. H. Radwan, K. K. A. Aziz, H. K. Hussein, A. E. Wakil and M. A. Hassan, "Silver nanoparticles instigate physiological, genotoxicity and ultrastructural anomalies in midgut tissues of beetles", *Chem. Biol. Interact.*, **2022**, *367*, Art.no.110166.
36. N. Saitou and M. Nei, "The neighbor-joining method: A new method for reconstructing phylogenetic trees", *Mol. Biol. Evol.*, **1987**, *4*, 406-425.
37. K. Tamura, M. Nei and S. Kumar, "Prospects for inferring very large phylogenies by using the neighbor-joining method" *Proc. Natl. Acad. Sci. U. S. A.*, **2004**, *101*, 11030-11035.
38. K. Tamura, G. Stecher and S. Kumar, "MEGA11: Molecular evolutionary genetics analysis version 11", *Mol. Biol. Evol.*, **2021**, *38*, 3022-3027.
39. K. S. Siddiqi, A. Husen and R. A. K. Rao, "A review on biosynthesis of silver nanoparticles and their biocidal properties", *J. Nanobiotechnol*., **2018**, *16*, Art.no.14.
40. S. Pasieczna-Patkowska, M. Cichy and J. Flieger, "Application of Fourier transform infrared (FTIR) spectroscopy in characterization of green synthesized nanoparticles", *Molecules*, **2025**, *30*, Art.no.684.

*Maejo Int. J. Sci. Technol.* **2026**, 20(03), 284-299

41. A. S. El-Hawary, O. M. Ibrahim, M. H. Kalaba, M. H. El-Sehrawy and M. K. A. Ismail, "*Limosilactobacillus fermentum*-derived silver nanoparticles: Biosynthesis, optimization, and biological activities", *Biomass Convers. Biorefine.*, **2025**, *15*, 9999-10013.
42. T. Ahmed, M. Shahid, M. Noman, M. B. K. Niazi, F. Mahmood, I. Manzoor, Y. Zhang, B. Li, Y. Yang, C. Yan and J. Chen, "Silver nanoparticles synthesized by using *Bacillus cereus* SZT1 ameliorated the damage of bacterial leaf blight pathogen in rice", *Pathogens*, **2020**, *9*, Art.no.160.
43. N. Kabeerdass, A. Al Otaibi, M. Rajendran, A. Manikandan, H. A. Kashmery, M. M. Rahman, P. Madhu, A. Khan, A. M. Asiri and M. Mathanmohun, "*Bacillus*-mediated silver nanoparticle synthesis and its antagonistic activity against bacterial and fungal pathogens", *Antibiotics*, **2021**, *10*, Art.no.1334.
44. Y. Luo and W. X. Wang, "Roles of hemocyte subpopulations in silver nanoparticle transformation and toxicity in the oysters *Crassostrea hongkongensis*", *Environ. Pollut.*, **2022**, *305*, Art.no.119281.

© 2026 by Maejo University, San Sai, Chiang Mai, 50290 Thailand. Reproduction is permitted for noncommercial purposes.